Pseudoscalar Meson Nonet at Zero and Finite Temperature[1]

D. Horvatić[*,2], D. Blaschke[†,‡,3], D. Klabučar[*,4], A. E. Radzhabov[‡,5],

[*] *Physics Department, Faculty of Science, University of Zagreb, Bijenička c. 32, Zagreb 10000, Croatia*
[†] *Institut für Physik, Universität Rostock D-18051 Rostock, Germany*
[‡] *Bogoliubov Laboratory of Theoretical Physics, Joint Institute for Nuclear Research, 141980 Dubna, Russia*

Abstract

Theoretical understanding of experimental results from relativistic heavy-ion collisions requires a microscopic approach to the behavior of QCD n-point functions at finite temperatures, as given by the hierarchy of Dyson-Schwinger equations, properly generalized within the Matsubara formalism. The convergence of sums over Matsubara modes is studied. The technical complexity of finite-temperature calculations mandates modeling. We present a model where the QCD interaction in the infrared, nonperturbative domain, is modeled by a separable form. Results for the mass spectrum of light quark flavors (u, d, s) and for the pseudoscalar bound-state amplitudes at finite temperature are presented.

1 Introduction

While the experiments at RHIC [1, 2] advanced the empirical knowledge of the hot QCD matter dramatically, the understanding of the state of matter that has been formed is still lacking. For example, the STAR collaboration's assessment [2] of the evidence from RHIC experiments depicts a very intricate, difficult-to-understand picture of the hot QCD matter. Among the issues pointed out as important was the need to clarify the role of quark-antiquark ($q\bar{q}$) bound states continuing existence above the critical temperature T_c, as well as the role of the chiral phase transition.

Both of these issues are consistently treated within the Dyson-Schwinger (DS) approach to quark-hadron physics. Dynamical chiral symmetry breaking (DChSB) as the crucial low-energy QCD phenomenon is well-understood in the rainbow-ladder approximation (RLA), a symmetry preserving truncation of the hierarchy of DS equations. Thanks to this, the behavior of the pion mass is in accord with the Goldstone theorem: the pion mass shows correct behavior while approaching the chiral limit, as seen on Fig. 1. This correct chiral behavior is a general feature of the DS approach in RLA, and not a consequence of our specific model choice. For recent reviews of the DS approach,

[1] Talk presented by D. Klabučar at the "Dense Matter In Heavy Ion Collisions and Astrophysics", JINR, Dubna, August 21 – September 1, 2006.

[2] davorh@phy.hr
[3] david@theor.jinr.ru
[4] klabucar@phy.hr, senior associate of Abdus Salam ICTP
[5] aradzh@theor.jinr.ru

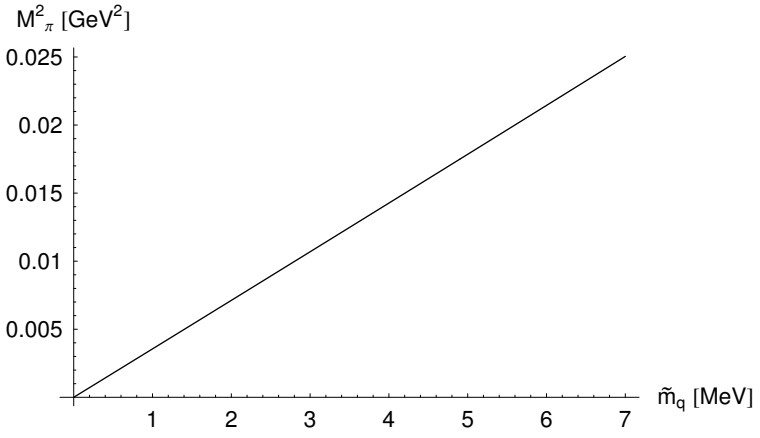

Figure 1: Correct chiral behavior of the pion mass close to chiral limit: $M_\pi^2 \propto \widetilde{m}_q$, where $\widetilde{m}_q$ is the bare quark mass parameter. It is akin to the notion of the current quark mass in QCD and gives the extent of the explicit chiral symmetry breaking as opposed to DChSB – see Eq. (1) below.

see, e.g., Refs. [3, 4], of which the first [3] also reviews the studies of QCD DS equations at finite temperature, started in [5]. Unfortunately, the extension of DS calculations to non-vanishing temperatures is technically quite difficult. This usage of separable model interactions greatly simplifies DS calculations at finite temperatures, while yielding equivalent results on a given level of truncation [6, 7]. A recent update of this covariant separable approach with application to the scalar σ meson at finite temperature can be found in [8]. Here, we present results for the quark mass spectrum at zero and finite temperature, extending previous work by including the strange flavor.

2 The separable model at zero temperature

The dressed quark propagator $S_q(p)$ is the solution of its DS equation [3, 4],

$$S_q(p)^{-1} = i\gamma\cdot p + \widetilde{m}_q + \frac{4}{3}\int \frac{d^4\ell}{(2\pi)^4}\, g^2 D^{\rm eff}_{\mu\nu}(p-\ell)\gamma_\mu S_q(\ell)\gamma_\nu\,, \qquad (1)$$

while the $q\bar{q}'$ meson Bethe-Salpeter (BS) bound-state vertex $\Gamma_{q\bar{q}'}(p,P)$ is the solution of the BS equation (BSE)

$$-\lambda(P^2)\Gamma_{q\bar{q}'}(p,P) = \frac{4}{3}\int \frac{d^4\ell}{(2\pi)^4} g^2 D^{\rm eff}_{\mu\nu}(p-\ell)\gamma_\mu S_q(\ell_+)\Gamma_{q\bar{q}'}(\ell,P)S_q(\ell_-)\gamma_\nu, \quad (2)$$

where $D^{\rm eff}_{\mu\nu}(p-\ell)$ is an effective gluon propagator modeling the nonperturbative QCD effects, $\widetilde{m}_q$ is the current quark mass, the index q (or q') stands for the quark flavor (u, d or s), P is the total momentum, and $\ell_\pm = \ell \pm P/2$. The

chiral limit is obtained by setting $\widetilde{m}_q = 0$. The meson mass is identified from $\lambda(P^2 = -M^2) = 1$. Equations (1) and (2) are written in the Euclidean space, and in the consistent rainbow-ladder truncation.

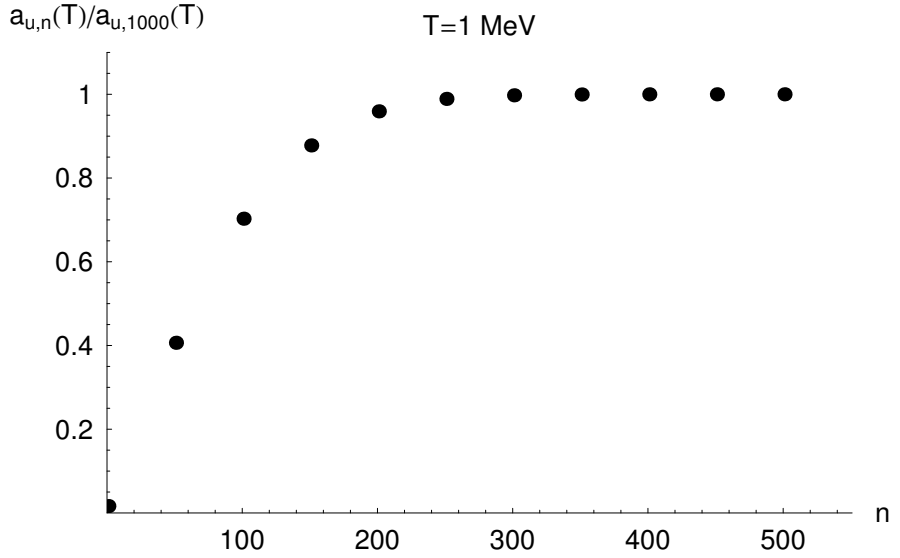

Figure 2: The sum in Eq. (8) as the function of number of the Matsubara modes included in summation at temperature $T = 1$ MeV. Eq. (8) is normalized to value calculated with enough Matsubara modes ($n = 1000$) to achieve prescribed numerical precision.

The simplest separable Ansatz which reproduces in RLA a nonperturbative solution of (1) for any effective gluon propagator in a Feynman-like gauge $g^2 D^{\rm eff}_{\mu\nu}(p-\ell) \to \delta_{\mu\nu} D(p^2, \ell^2, p\cdot\ell)$ is [6, 7]

$$D(p^2, \ell^2, p\cdot\ell) = D_0 \mathcal{F}_0(p^2)\mathcal{F}_0(\ell^2) + D_1 \mathcal{F}_1(p^2)(p\cdot\ell)\mathcal{F}_1(\ell^2)\ . \tag{3}$$

This is a rank-2 separable interaction with two strength parameters D_i and corresponding form factors $\mathcal{F}_i(p^2)$, $i = 1, 2$. The choice for these quantities is constrained to the solution of the DSE for the quark propagator (1)

$$S_q(p)^{-1} = i\gamma\cdot p A_q(p^2) + B_q(p^2) \equiv Z_q^{-1}(p^2)[i\gamma\cdot p + m_q(p^2)]\ , \tag{4}$$

where $m_q(p^2) = B_q(p^2)/A_q(p^2)$ is the dynamical mass function and $Z_q(p^2) = A_q^{-1}(p^2)$ the wave function renormalization. Using the separable Ansatz (3) in (1), the gap equations for the quark amplitudes $A_q(p^2)$ and $B_q(p^2)$ read

$$B_q(p^2) - \widetilde{m}_q = \frac{16}{3}\int \frac{d^4\ell}{(2\pi)^4} D(p^2, \ell^2, p\cdot\ell)\frac{B_q(\ell^2)}{\ell^2 A_q^2(\ell^2) + B_q^2(\ell^2)} = b_q \mathcal{F}_0(p^2)\,, \tag{5}$$

$$\big[A_q(p^2) - 1\big] = \frac{8}{3p^2}\int \frac{d^4\ell}{(2\pi)^4} D(p^2, \ell^2, p\cdot\ell)\frac{(p\cdot\ell)A_q(\ell^2)}{\ell^2 A_q^2(\ell^2) + B_q^2(\ell^2)} = a_q \mathcal{F}_1(p^2)\,. \tag{6}$$

Once the coefficients a_q and b_q are obtained by solving the gap equations (5) and (6), the only model parameters remaining are $\widetilde{m}_q$ and the parameters of the gluon propagator, to be fixed by meson phenomenology.

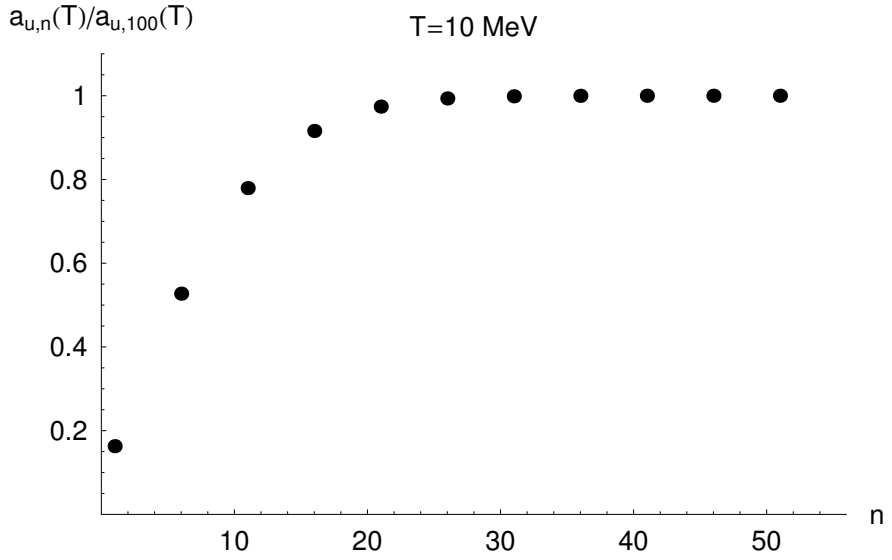

Figure 3: The sum in Eq. (8) as the function of number of the Matsubara modes included in summation at temperature $T = 10$ MeV. Eq. (8) is normalized to value calculated with enough Matsubara modes ($n = 100$) to achieve prescribed numerical precision.

3 Extension to finite temperature

The extension of the separable model studies to the finite temperature case, $T \neq 0$, is systematically accomplished by a transcription of the Euclidean quark 4-momentum via $p \to p_n = (\omega_n, \vec{p})$, where $\omega_n = (2n+1)\pi T$ are the discrete Matsubara frequencies. In the Matsubara formalism, the number of coupled equations represented by (1) and (2) scales up with the number of fermion Matsubara modes included. For studies near and above the transition, $T \geq 100$ MeV, using only 10 such modes appears adequate. Nevertheless, the appropriate number can be more than 10^3 if the continuity with $T = 0$ results is to be verified. Convergence of the sum in the Eq. (8) is shown on Figs. 2–4. The effective $\bar{q}q$ interaction, defined in the present paper by the Ansatz (3) and the form factors (12) below, will automatically decrease with increasing T without the introduction of an explicit T-dependence which would require new parameters.

The solution of the DS equation for the dressed quark propagator now takes the form

$$S_q^{-1}(p_n, T) = i\vec{\gamma} \cdot \vec{p}\, A_q(p_n^2, T) + i\gamma_4 \omega_n\, C_q(p_n^2, T) + B_q(p_n^2, T), \qquad (7)$$

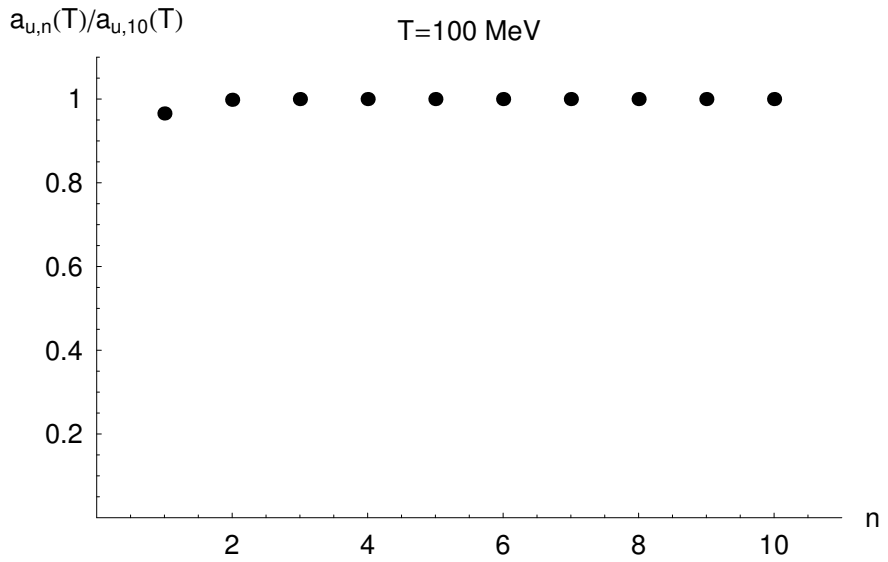

Figure 4: The sum in the Eq. (8) as function of number of the Matsubara modes included in summation at temperature $T = 100$ MeV. Eq. (8) is normalized to value calculated with enough Matsubara modes ($n = 10$) to achieve prescribed numerical precision.

where $p_n^2 = \omega_n^2 + \vec{p}^{\,2}$ and the quark amplitudes $B_q(p_n^2, T) = \widetilde{m}_q + b_q(T)\mathcal{F}_0(p_n^2)$, $A_q(p_n^2, T) = 1 + a_q(T)\mathcal{F}_1(p_n^2)$, and $C_q(p_n^2, T) = 1 + c_q(T)\mathcal{F}_1(p_n^2)$ are defined by the temperature-dependent coefficients $a_q(T)$,$b_q(T)$, and $c_q(T)$ to be determined from the set of three coupled non-linear equations

$$a_q(T) = \frac{8D_1}{9}\, T \sum_n \int \frac{d^3p}{(2\pi)^3}\, \mathcal{F}_1(p_n^2)\, \vec{p}^{\,2}\, [1 + a_q(T)\mathcal{F}_1(p_n^2)]\; d_q^{-1}(p_n^2, T)\;, \tag{8}$$

$$c_q(T) = \frac{8D_1}{3}\, T \sum_n \int \frac{d^3p}{(2\pi)^3}\, \mathcal{F}_1(p_n^2)\, \omega_n^2\, [1 + c_q(T)\mathcal{F}_1(p_n^2)]\; d_q^{-1}(p_n^2, T)\;, \tag{9}$$

$$b_q(T) = \frac{16D_0}{3}\, T \sum_n \int \frac{d^3p}{(2\pi)^3}\, \mathcal{F}_0(p_n^2)\, [\widetilde{m}_q + b_q(T)\mathcal{F}_0(p_n^2)]\; d_q^{-1}(p_n^2, T)\;. \tag{10}$$

The function $d_q(p_n^2, T)$ is the denominator of the quark propagator $S_q(p_n, T)$, and is given by

$$d_q(p_n^2, T) = \vec{p}^{\,2} A_q^2(p_n^2, T) + \omega_n^2 C_q^2(p_n^2, T) + B_q^2(p_n^2, T). \tag{11}$$

The procedure for solving gap equations for a given temperature T is the same as in $T = 0$ case, but one has to control the appropriate number of Matsubara modes as mentioned above.

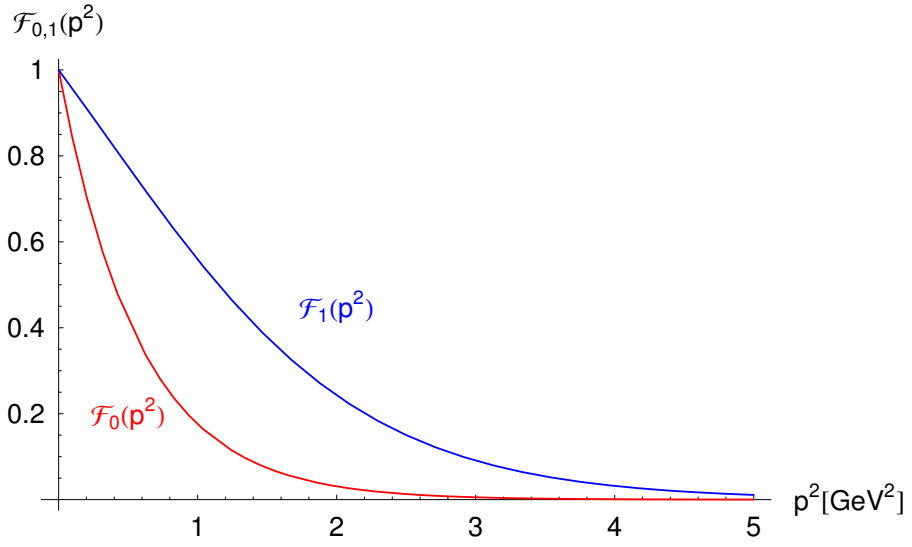

Figure 5: The p^2 dependence of the form factors $\mathcal{F}_0(p^2)$ and $\mathcal{F}_1(p^2)$.

4 Confinement and Dynamical Chiral Symmetry Breaking

If there are no poles in the quark propagator $S_q(p)$ for real timelike p^2 then there is no physical quark mass shell. This entails that quarks cannot propagate freely, and the description of hadronic processes will not be hindered by unphysical quark production thresholds. This sufficient condition is a viable possibility for realizing quark confinement [7]. A nontrivial solution for $B_q(p^2)$ in the chiral limit ($\widetilde{m}_0 = 0$) signals DChSB. There is a connection between quark confinement realized as the lack of a quark mass shell and the existence of a strong quark mass function in the infrared through DChSB. The propagator is confining if $m_q^2(p^2) \neq -p^2$ for real p^2, where the quark mass function is $m_q(p^2) = B_q(p^2)/A_q(p^2)$. In the present separable model, the strength $b_q = B_q(0)$, which is generated by solving Eqs. (5) and (6), controls both confinement and DChSB. At finite temperature, the strength $b_q(T)$ for the quark mass function will decrease with T, until the denominator (11) of the quark propagator can vanish for some timelike momentum, and the quark can come on the free mass shell. The connection between deconfinement and disappearance of DChSB is thus clear in the DS approach. Also the present model is therefore expected to have a deconfinement transition at or a little before the chiral restoration transition associated with $b_0(T) \to 0$.

The following simple choice of the separable interaction form factors (graphically represented on Fig. 5),

$$\mathcal{F}_0(p^2) = \exp(-p^2/\Lambda_0^2) \ , \quad \mathcal{F}_1(p^2) = \frac{1+\exp(-p_0^2/\Lambda_1^2)}{1+\exp((p^2-p_0^2)/\Lambda_1^2)} \ , \tag{12}$$

is used to obtain numerical solutions which reproduce very well the phenomenology of the light pseudoscalar mesons and generate an acceptable value for the chiral condensate.

The resulting quark propagator is found to be confining and the infrared strength and shape of quark amplitudes $A_q(p^2)$ and $B_q(p^2)$ are in quantitative agreement with the typical DS studies. Gaussian-type form factors are used as a minimal way to preserve these properties while realizing that the ultraviolet suppression is much stronger than the asymptotic fall off (with logarithmic corrections) known from perturbative QCD and numerical studies on the lattice [9].

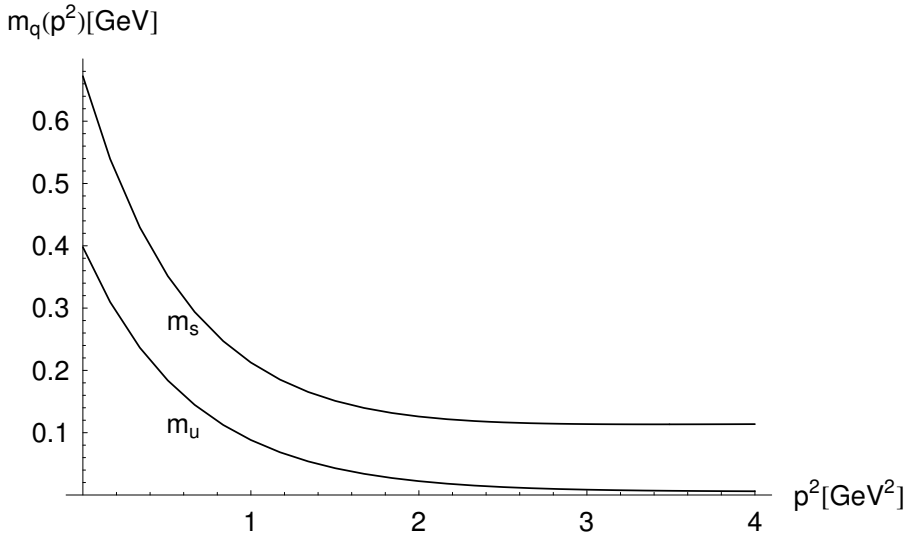

Figure 6: The p^2 dependence (at $T = 0$) of the dynamically generated quark masses $m_s(p^2), m_u(p^2)$ for, respectively, the strange and the (isosymmetric) non-strange case.

5 Bound-state amplitudes

With the separable interaction, the allowed form of the solution of Eq. (2) for the pseudoscalar BS amplitude is [6]

$$\Gamma_{PS}(\ell; P) = \gamma_5 \left(iE_{PS}(P^2) + \not{P} F_{PS}(P^2) \right) \mathcal{F}_0(\ell^2). \tag{13}$$

The dependence on the relative momentum ℓ is described only by the first form factor $\mathcal{F}_0(\ell^2)$. The second term $\mathcal{F}_1$ of the interaction can contribute to BS amplitude only indirectly via the quark propagators. The pseudoscalar BSE (2) becomes a 2×2 matrix eigenvalue problem $\mathcal{K}(P^2)\mathcal{V} = \lambda(P^2)\mathcal{V}$ where the

eigenvector is $\mathcal{V} = (E_{PS}, F_{PS})$. The kernel is

$$\mathcal{K}_{ij}(P^2) = -\frac{4D_0}{3}\,\mathrm{tr_s}\int \frac{d^4\ell}{(2\pi)^4}\mathcal{F}_0^2(\ell^2)\left[\hat{t}_i\, S_q(\ell_+)\, t_j\, S_{\bar{q}}(\ell_-)\right] \ , \tag{14}$$

where $i,j = 1,2$ denote the components of $t = (i\gamma_5, \gamma_5 \not{P})$ and $\hat{t} = (i\gamma_5, -\gamma_5 \not{P}/2P^2)$. The separable model produces the same momentum dependence for both amplitudes (containing F_{PS} and E_{PS}) in the BS amplitude (13): the dependence of the quark amplitude $B_q(\ell^2)$. Goldstone's theorem is preserved by the present separable model; in the chiral limit, whenever a nontrivial gap-equation solution for $B_q(p^2)$ exists, there will be a massless pion solution to (14).

The normalization condition for the pseudoscalar BS amplitude can be expressed as

$$\begin{aligned} 2P_\mu &= N_f N_c \frac{\partial}{\partial P_\mu}\int \frac{d^4\ell}{(2\pi)^4}\,\mathrm{tr}_s\left[\bar{\Gamma}_{PS}(\ell;-K)\ \times\right. \\ &\times \left. S_q(\ell_+)\,\Gamma_{PS}(\ell;K)\,S_{\bar{q}}(\ell_-)\right]|_{P^2=K^2=-M_{PS}^2}\,. \end{aligned} \tag{15}$$

Here $\bar{\Gamma}(q;K)$ is the charge conjugate amplitude $[\mathcal{C}^{-1}\Gamma(-q,K)\mathcal{C}]^{\mathrm{t}}$, where $\mathcal{C} = \gamma_2\gamma_4$ and the index t denotes a matrix transpose. Both the number of colors N_c and light flavors N_f are 3.

At $T = 0$ the mass-shell condition for a meson as a $\bar{q}q$ bound state of the BSE is equivalent to the appearance of a pole in the $\bar{q}q$ scattering amplitude as a function of P^2. At $T \neq 0$ in the Matsubara formalism, the $O(4)$ symmetry is broken by the heat bath and we have $P \to (\Omega_m, \vec{P})$ where $\Omega_m = 2m\pi T$. Bound states and the poles they generate in propagators may be investigated through polarization tensors, correlators or Bethe-Salpeter eigenvalues. This pole structure is characterized by information at discrete points Ω_m on the imaginary energy axis and at a continuum of 3-momenta. One may search for poles as a function of $\vec{P}^2$ thus identifying the so - called spatial or screening masses for each Matsubara mode. These serve as one particular characterization of the propagator and the $T > 0$ bound states.

In the present context, the eigenvalues of the BSE become $\lambda(P^2) \to \tilde{\lambda}(\Omega_m^2, \vec{P}^2; T)$. The temporal meson masses identified by zeros of $1 - \tilde{\lambda}(\Omega^2, 0; T)$ will differ in general from the spatial masses identified by zeros of $1 - \tilde{\lambda}(0, \vec{P}^2; T)$. They are however identical at $T = 0$ and an approximate degeneracy can be expected to extend over the finite T domain, where the $O(4)$ symmetry is not strongly broken.

The general form of the finite-T pseudoscalar BS amplitude allowed by the separable model is

$$\begin{aligned} \Gamma_{PS}(q_n;P_m) &= \gamma_5\left(iE_{PS}(P_m^2) + \gamma_4\,\Omega_m\tilde{F}_{PS}(P_m^2)\right. \\ &+ \left.\vec{\gamma}\cdot\vec{P}F_{PS}(P_m^2)\right)\ \mathcal{F}_0(q_n^2)\,. \end{aligned} \tag{16}$$

The separable BSE becomes a 3×3 matrix eigenvalue problem with a kernel that is a generalization of Eq. (14). In the limit $\Omega_m \to 0$, as is required for the spatial mode of interest here, the amplitude $\hat{F}_{PS} = \Omega_m\tilde{F}_{PS}$ is trivially zero.

6 Results

Parameters of the model are completely fixed by meson phenomenology calculated from the model as discussed in [7, 8]. In the nonstrange sector, we work in the isosymmetric limit and adopt bare quark masses $\widetilde{m}_u = \widetilde{m}_d = 5.5$ MeV and in strange sector we adopt $\widetilde{m}_s = 115$ MeV. Then the parameter values

$$\Lambda_0 = 758\,\mathrm{MeV}, \quad \Lambda_1 = 961\,\mathrm{MeV}, \quad p_0 = 600\,\mathrm{MeV}, \tag{17}$$

$$D_0\Lambda_0^2 = 219\,, \qquad D_1\Lambda_1^4 = 40\,, \tag{18}$$

lead, through the gap equation, to $a_{u,d} = 0.672$, $b_{u,d} = 660$ MeV, $a_s = 0.657$ and $b_s = 998$ MeV i.e., to the dynamically generated momentum-dependent mass functions $m_q(p^2)$ shown in Fig. 6. In the limit of high p^2, they converge to $\widetilde{m}_u$ and $\widetilde{m}_s$. However, at low p^2, the values of $m_u(p^2)$ are close to the typical constituent quark mass scale $\sim m_\rho/2 \sim m_N/3$ with the maximum value at $p^2 = 0$, $m_u(0) = 398$ MeV. The corresponding value for the strange quark is $m_s(0) = 672$ MeV. Fig. 6 hence shows that in the domain of low and intermediate $p^2 \lesssim 1$ GeV^2, the dynamically generated quark masses are of the order of typical constituent quark mass values.

Thus, the DS approach provides a derivation of the constituent quark model [10] from a more fundamental level, with the correct chiral behavior of QCD.

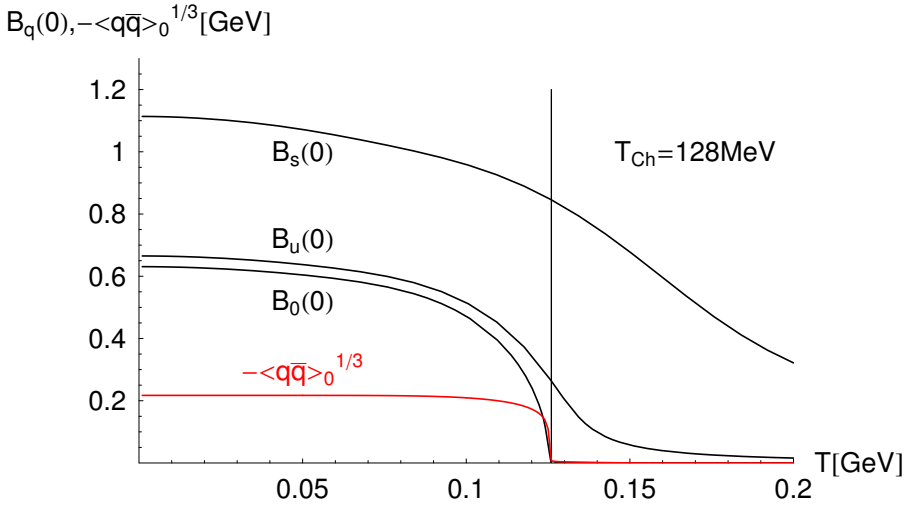

Figure 7: The temperature dependence of $B_s(0), B_u(0)$ and $B_0(0)$, the scalar propagator functions at $p^2 = 0$, for the strange, the nonstrange and the chiral-limit cases, respectively. The temperature dependence of the chiral quark-antiquark condensate, $-\langle q\bar{q}\rangle_0^{1/3}$, is also shown (by the lowest curve). Both chiral-limit quantities, $B_0(0)$ and $-\langle q\bar{q}\rangle_0^{1/3}$, vanish at the chiral-symmetry restoration temperature $T_{\rm Ch} = 128$ MeV.

Obtaining such dynamically generated constituent quark masses, as previous experience with the DS approach shows (see, e.g., Refs. such as [3, 4, 10]), is essential for reproducing the static and other low-energy properties of hadrons, including decays. (We would have to turn to less simplified DS models for incorporating the correct perturbative behaviors, including that of the quark masses. Such models are amply reviewed or used in, e.g., Refs. [3, 4, 10, 11], but addressing them is beyond the present scope, where the perturbative regime is not important.)

Another important result related to the dynamically generated, dressed quark propagator, is the chiral quark-antiquark condensate $\langle q\bar{q}\rangle_0$. For the parameter values quoted above, we obtain the zero-temperature value $\langle q\bar{q}\rangle_0 = (-217\,\mathrm{MeV})^3$, which practically coincides with the standard QCD value.

The extension of these results to finite temperatures is given in Figs. 7, 8. Very important is the temperature dependence of the chiral-limit quantities $B_0(0)_T$ and $\langle q\bar{q}\rangle_0(T)$, whose vanishing with T determines the chiral restoration temperature T_{Ch}. We find $T_{\mathrm{Ch}} = 128$ MeV in the present model.

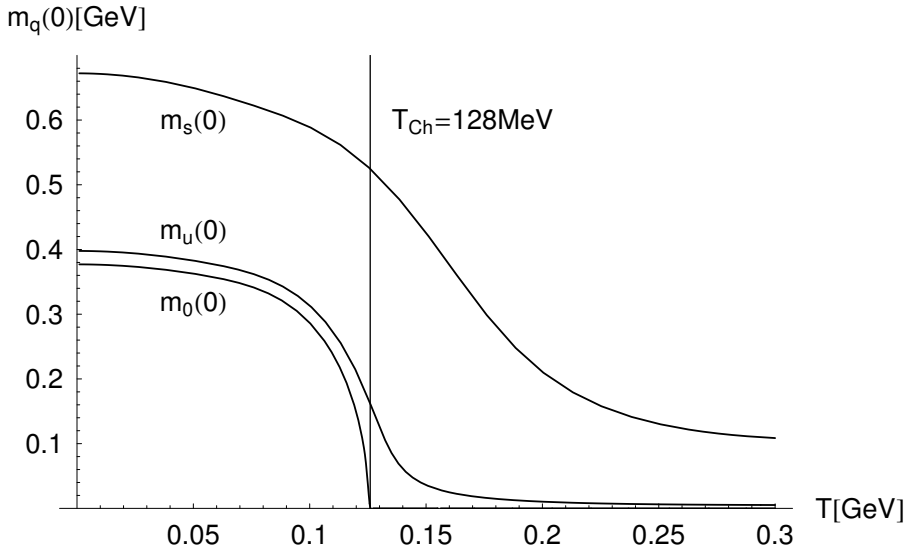

Figure 8: The temperature dependence of $m_s(0), m_u(0)$ and $m_0(0)$, the dynamically generated quark masses at $p^2 = 0$ for the strange, the nonstrange and the chiral-limit cases, respectively.

The temperature dependences of the functions giving the vector part of the quark propagator, $A_{u,s}(0)_T$ and $C_{u,s}(0)_T$, are depicted in Fig. 9. Their difference is a measure of the O(4) symmetry breaking with the temperature T.

The results for pseudoscalar E_{PS} and pseudovector F_{PS} amplitudes can be seen on Fig. 10. The pseudovector amplitude for pion F_π is significantly different from zero but decreases rapidly above the transition.

The presented model, when applied in the framework of the Bethe-Salpeter approach to mesons as quark-antiquark bound states, produces a very satisfac-

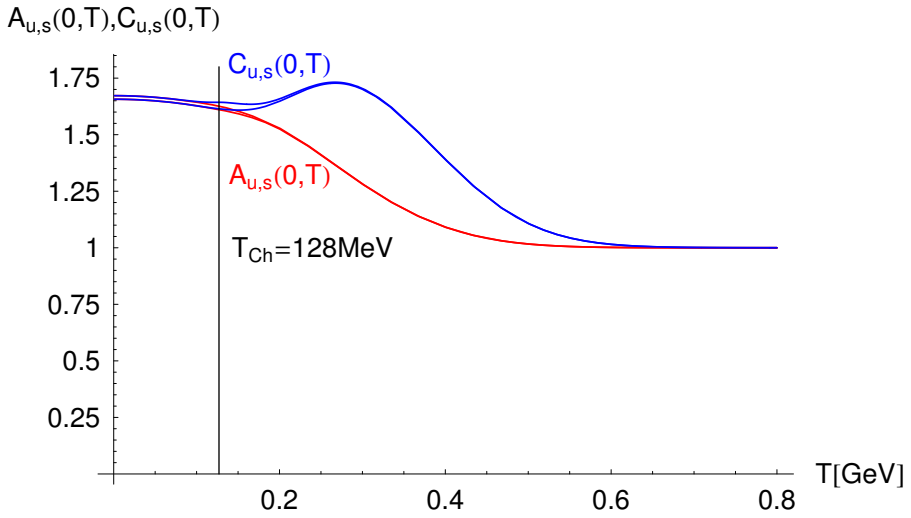

Figure 9: The violation of $O(4)$ symmetry with T is exhibited on the example of $A_{u,s}(0,T)$ and $C_{u,s}(0,T)$.

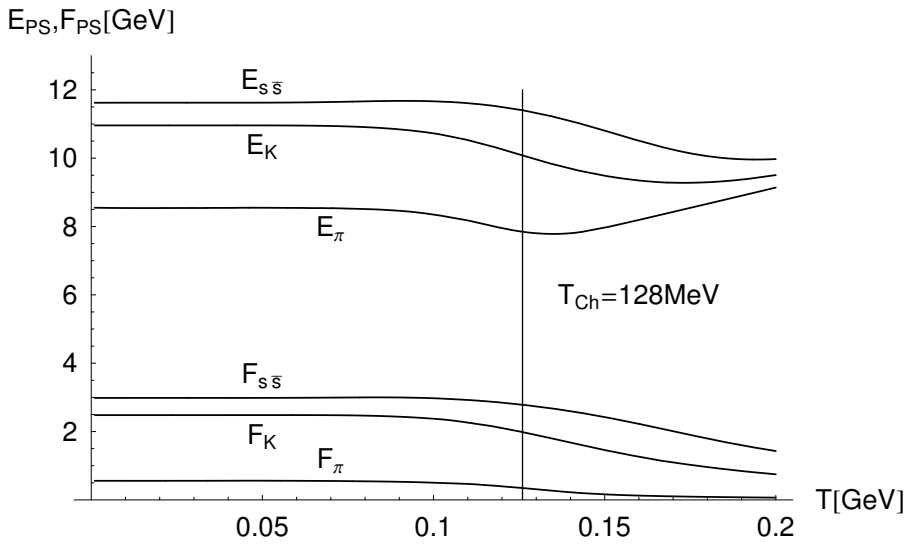

Figure 10: The temperature dependence of pseudoscalar covariants in BS amplitude

tory description of the whole light pseudoscalar nonet, both at zero and finite temperatures [12]. The masses and decay constants of the pseudoscalar nonet mesons at $T = 0$ are summarized and compared with experiment in Table 1.

The first three rows in Table 1 give the masses M_{PS} and decay constants f_{PS} of the pseudoscalar $q\bar{q}'$ bound states $PS = \pi^+, K^+$, and $s\bar{s}$ resulting, through the BS equation (2), from the separable interaction (3). The $s\bar{s}$ pseudoscalar meson is a useful theoretical construct, but is not realized physically, at least not at $T = 0$. (It is therefore not associated with any experimental value in this table. Also note that the unphysical mass $M_{s\bar{s}}$ given in this table does not include the contribution from the gluon anomaly.) The parameter values [(17) and (18) in the effective interaction $D^{\rm eff}_{\mu\nu}$, and the bare quark masses $\widetilde{m}_{u,d} = 5.5$ MeV and $\widetilde{m}_s = 115$ MeV] are fixed by fitting the pion and kaon masses and decay constants. These masses and decay constants are the input for the description of the η–η' complex [11]. More precisely, η and η' masses are obtained by combining the contributions from the non-Abelian (gluon) axial anomaly with the non-anomalous contributions obtained from the results on the masses of π, K, and the unphysical $s\bar{s}$ pseudoscalar [11]. For this procedure, it is essential that we have the good chiral behavior of our $q\bar{q}'$ bound states, which are simultaneously also the (almost-)Goldstone bosons, so that

$$M^2_{q\bar{q}'} = \text{Const}\,(\widetilde{m}_q + \widetilde{m}_{q'})\,, \tag{19}$$

as seen in Fig. 1. For example, Eq. (19) guarantees the relation $M^2_\pi + M^2_{s\bar{s}} = 2M^2_K$ which is utilized in Refs. [11, 12] in the treatment of the η-η' complex. Indeed, the concrete model results for M_π, M_K and $M_{s\bar{s}}$ in Table 1 obey this relation up to $\frac{1}{4}\%$.

PS	M_{PS}	$M^{\rm exp}_{PS}$	f_{PS}	$f^{\rm exp}_{PS}$
π^+	0.140	0.1396	0.092	0.0924 ± 0.0003
K^+	0.495	0.4937	0.110	0.1130 ± 0.0010
$s\bar{s}$	0.685		0.119	
η	0.543	0.5473		
η'	0.933	0.9578		

Table 1: Results on the pseudoscalar mesons at zero temperature, $T = 0$, and comparison with experiment (where appropriate). All results are in GeV.

Especially interesting is the temperature behavior of the η-η' complex, where the results for the meson masses differ very much for various possible relationships between the chiral restoration temperature $T_{\rm Ch}$ and the temperature of melting of the topological susceptibility, denoted by T_χ. The once favored scenario of Pisarski and Wilczek [14], where η would smoothly evolve with T to purely non-strange η_{NS},

$$|\eta_{NS}\rangle = \frac{1}{\sqrt{2}}(|u\bar{u}\rangle + |d\bar{d}\rangle) = \frac{1}{\sqrt{3}}|\eta_8\rangle + \sqrt{\frac{2}{3}}|\eta_0\rangle\ , \tag{20}$$

and η' to purely strange η_S,

$$|\eta_S\rangle = |s\bar{s}\rangle = -\sqrt{\frac{2}{3}}|\eta_8\rangle + \frac{1}{\sqrt{3}}|\eta_0\rangle\ , \tag{21}$$

would occur only when T_χ is significantly below $T_{\rm Ch}$. Such a case is depicted in Fig. 11, where $T_\chi = 2/3\,T_{\rm Ch}$. In this case, around the chiral restoration temperature η becomes quite light, and one would expect an increase of the relative multiplicity of η mesons around $T_{\rm Ch}$. Nevertheless, the possibility that $T_\chi < T_{\rm Ch}$ is nowadays disfavored by the lattice results on the temperature dependence of the topological susceptibility [13].

On the other hand, for $T_\chi \sim T_{\rm Ch}$ or $T_\chi > T_{\rm Ch}$ we find that η never becomes light, while η' even becomes very heavy [12]. Thus, for the relationships favored by the lattice, our results [12] indicate so strong suppression of η' around the chiral restoration temperature, that it may constitute a useful signal from the hot QCD matter.

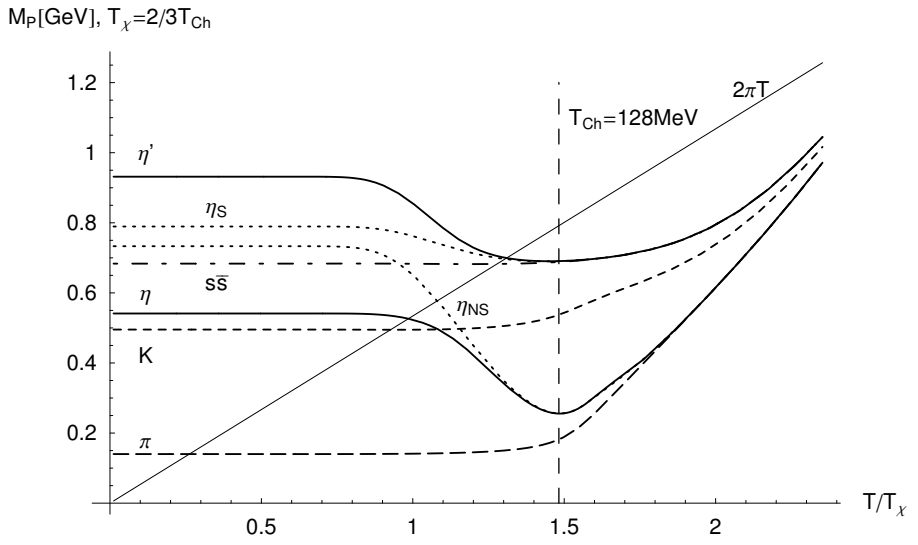

Figure 11: The relative temperature dependence, on T/T_χ, of the pseudoscalar meson masses for $T_\chi = 2/3\,T_{\rm Ch}$. The three variously dashed curves represent the pseudoscalar meson masses which do not receive contributions from the gluon anomaly: $M_\pi(T)$, $M_K(T)$ and $M_{s\bar{s}}(T)$, depicted by the long-dashed, short dashed and dash-dotted curves, respectively. The lower solid curve is $M_\eta(T)$, and the upper solid curve is $M_{\eta'}(T)$. The lower and upper dotted curves are the masses of η_{NS} and η_S. The thin diagonal line is twice the zeroth Matsubara frequency, $2\pi T$. This is the limit to which meson masses should ultimately approach from below at still higher temperatures, where $q\bar{q}$ states should totally dissolve into a gas of weakly interacting quarks and antiquarks.

Acknowledgments

We thank M. Bhagwat, Yu.L. Kalinovsky and P.C. Tandy for discussions. A.E.R. acknowledges support by RFBR grant No. 05-02-16699, the Heisenberg-Landau program and the HISS Dubna program of the Helmholtz Association. D.H. and D.K.

were supported by MZT project No. 0119261. D.B. is grateful for support by the Croatian Ministry of Science for a series of guest lectures held in the Physics Department at University of Zagreb, where the present work has been completed. D.K. acknowledges the partial support of Abdus Salam ICTP at Trieste, where a part of this paper was written.

References

[1] *Müller B. and Nagle J. L.* // Ann. Rev. Nucl. Part. Systems 2006. V.56 P.93.

[2] *Adams J. et al. [STAR Collaboration]* // Nucl. Phys. A. 2005. V.757. P.102.

[3] *Roberts C. D. and Schmidt S. M.* // Prog. Part. Nucl. Phys. 2000. V.45. S.1.

[4] *Alkofer R. and Smekal R.* // Phys. Rept. 2001. V.353. P.281.

[5] *Bender A., Blaschke D., Kalinovsky Y. and Roberts C. D.* // Phys. Rev. Lett. 1996. V.77. P.3724.

[6] *Burden C. J., Qian L., Roberts C. D., Tandy P. C. and Thomson M. J.* // Phys. Rev. C. 1997. V.55. P.2649.

[7] *Blaschke D., Burau G., Kalinovsky Yu. L., Maris P. and Tandy P. C.* // Int. J. Mod. Phys. A. 2001. V.16. P.2267.

[8] *Blaschke D., Kalinovsky Yu. L., Radzhabov A. E. and Volkov M. K.* // Phys. Part. Nucl. Lett. 2006. V.3. P.327.

[9] *Parappilly M. B., Bowman P. O., Heller U. M., Leinweber D. B., Williams A. G. and Zhang J. B.* // Phys. Rev. D. 2006. V.73. P.054504.

[10] *Kekez D., Bistrović B. and Klabučar D.* // Int. J. Mod. Phys. A. 1999. V.14. P.161;
Kekez D., Klabučar D. and Scadron M. D. // J. Phys. G. 2000. V.26. P.1335.

[11] *Klabučar D. and Kekez D.* // Phys. Rev. D. 1998. V.58. P.096003;
Klabučar D. and Kekez D. // Phys. Rev. D. 2002. V.65. P.057901;
Klabučar D. and Kekez D. // Phys. Rev. D. 2006. V.73. P.036002.

[12] *Blaschke D., Horvatić D., Klabučar D. and Radzhabov A. E.* // Zagreb University preprint ZTF-06-10-1.

[13] *Alles B., D'Elia M. and Di Giacomo A.* // Nucl. Phys. B. 1997. V.494 P.281;
Alles B. and D'Elia M. // arXiv:hep-lat/0602032.

[14] *Pisarski R. D. and Wilczek F.* // Phys. Rev. D. 1984. V.29 P.338.